Chemistry Central Journal

ChemistryCentral

Research article

Open Access

Characterization of deposits formed on diesel injectors in field test and from thermal oxidative degradation of n-hexadecane in a laboratory reactor

Ramya Venkataraman[1] and Semih Eser*[2]

Address: [1]Department of Energy and Geo-Environmental Engineering, The Pennsylvania State University, University Park, Pennsylvania 16802, USA and [2]Department of Energy and Mineral Engineering, The Pennsylvania State University, University Park, Pennsylvania16802, USA

E-mail: Ramya Venkataraman - ramya_vnkt@yahoo.com; Semih Eser* - seser@psu.edu;
*Corresponding author

Published: 17 December 2008

Chemistry Central Journal 2008, **2**:25 doi: 10.1186/1752-153X-2-25

Received: 29 July 2008

Accepted: 17 December 2008

This article is available from: http://journal.chemistrycentral.com/content/2/1/25

Abstract

Solid deposits from commercially available high-pressure diesel injectors (HPDI) were analyzed to study the solid deposition from diesel fuel during engine operation. The structural and chemical properties of injector deposits were compared to those formed from the thermal oxidative stressing of a diesel fuel range model compound, n-hexadecane at 160°C and 450 psi for 2.5 h in a flow reactor. Both deposits consist of polyaromatic compounds (PAH) with oxygen moieties. The similarities in structure and composition of the injector deposits and n-hexadecane deposits suggest that laboratory experiments can simulate thermal oxidative degradation of diesel in commercial injectors. The formation of PAH from n-hexadecane showed that aromatization of straight chain alkanes and polycondensation of aromatic rings was possible at temperatures as low as 160°C in the presence of oxygen. A mechanism for an oxygen-assisted aromatization of cylcoalkanes is proposed.

Background

Diesel fuel has a widespread use in engines that vary in size, speed, power output and application. This includes all forms of land and sea transportation, power generation units and machinery for industrial use. The thermal stability of diesel is therefore a critical parameter for the smooth operation of these systems. Filter plugging and solid deposit formation on fuel injector tips are the two problems most commonly encountered among diesel engine operators. The formation of deposits has been attributed to diesel instability during storage and engine operation [1]. These deposits can cause serious malfunction or even failure in extreme cases. One important feature that distinguishes jet fuel and diesel from gasoline is that their chemical composition allows them to be self igniting. The diesel instability problem is worsened by the presence of relatively longer chain paraffins in the fuel.

Studies so far have shown that fuel oxidation products, hydroperoxides and alkylperoxy radicals are primarily responsible for the formation of insoluble deposits from diesel and other middle distillates [1, 2]. Solid and liquid products formed from the thermal oxidative degradation of jet fuel were characterized in the previous chapter. This study investigates the nature of HPDI deposits obtained from high-pressure fuel injector, comparing these deposits with those formed from jet fuel. Since information on the hydrocarbon and heteroatom composition of the batch of diesel fuel from which these solids were formed was not available, deposits obtained from the stressing of a model compound (n-hexadecane) were characterized and compared in order to glean the thermal history and formation mechanism of the injector deposits.

Results and discussion

The thermal stressing conditions to which the diesel fuel was subjected in the injectors were not known. The results of the chemical and morphological analysis of these deposits are discussed in this section, along with the results obtained from n-hexadecane stressing experiments.

GC/MS analysis of liquid soluble components

The injector deposits scraped from the tip were washed in a 50% methanol – 50% pentane mixture, at a concentration of 25 mg of solid in 1 mL of liquid. The GC/MS chromatogram of these liquid-soluble compounds is shown in Figure 1. Additional file 1 lists the most likely assignments for the compounds in the solution. This showed the presence of significant amounts of alkyl-hydroperoxides, aldehydes, ketones, alcohols, ethers and acids. These compounds are known to form during the thermal oxidative degradation of middle distillates. In the case of diesel, they can form at temperatures as low as 45°C (during storage) up to 250°C (during engine operation) [1].

Similar oxygenated compounds were also seen in the GC/MS spectrum of liquid degradation products formed from the thermal oxidative degradation of jet fuel [3] with the primary difference being the length of the alkyl chain. With diesel being comprised of longer hydrocarbon chains (C_{14} – C_{21}) as compared to jet fuel (C_8 – C_{17}) the length of the corresponding oxygenated compounds formed from diesel degradation is also higher. The presence of the oxygenated straight chain compounds is attributed to the intermediate products formed from the free radical mechanisms leading to the thermal oxidative degradation of middle distillates [1, 4].

The pentane soluble fractions consisted of C_{19} – C_{27} straight and branched chain alkanes. These are clearly formed from scission and recombination reactions of the hydrocarbon chains present in diesel fuel. Such compounds as 1-(2-hydroxypropyl) naphthalene [5] are good indicators of the presence of oxygenated cyclic intermediates formed by low-temperature isomerization and cyclization reactions during the thermal oxidative degradation of diesel fuel. Some oxygenated impurities such as bis(1-methylpropyl) ester ethanoic acid and diesel additives were also identified in the GC/MS spectra of the liquid phase products [6]. The impurities identified are mostly from synthetic lubricating oil used in diesel engines.

A small fraction of the solid deposits removed from the nozzle tip dissolved in toluene. The GC/MS analysis of this solution revealed compounds like mono, di, and tri-substituted benzenes, 1 and 2 ring substituted cycloalkanes, and naphthalene. These compounds are considered to be liquid degradation products adsorbed on the solid deposits. Vacuum drying at 200°C for 2 h removed most of these adsorbed liquids.

Pyrolysis GC/MS of the deposits helped identify more than 200 compounds. A significant portion of the fragmentation products were benzene and alkylated benzenes. The largest ion seen in a mass spectrum profile of the deposits was coronene – a seven-ring condensed polyaromatic compound. These observations provide further evidence that the deposits consist of relatively large polyaromatic hydrocarbons (with H/C < 0.5) and explain why a large fraction of the solid deposits does not dissolve in liquid solvents.

The MALDI analysis was done to obtain the molecular weight distribution of these aromatic solids. The MALDI spectrum of these deposits in Figure 2 showed a molecular weight distribution of 82 to 1000 amu indicating that the largest constituents may contain up

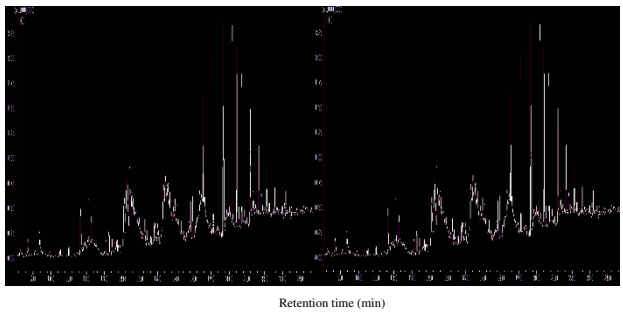

Figure 1
GC/MS chromatogram of 50% pentane – 50% methanol solubles from HPDI deposits.

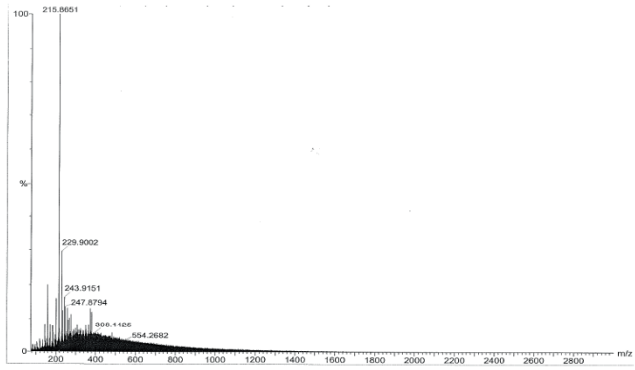

Figure 2
MALDI spectrum of HPDI deposits.

to fourteen condensed aromatic rings. The compound with a mass of 82 amu (at very low concentration in this sample) is most likely methyl furan. The highest fraction of the deposits seemed to be a homologous series of pyrene starting at a mass of 202 amu. The mass addition of 14 corresponds to the addition of a methyl group to pyrene. Coronene with a molecular weight of 300 amu lies in the middle of the molecular weight range of these deposits.

Examination of microstructure of deposits

The deposits obtained from the tip of the diesel injector nozzles include loose powdery material resembling soot, similar to deposits formed from the thermal oxidative degradation of jet fuel [3]. In Figure 3, FESEM images show that the HPDI deposits consist of clusters of spherical particles. They form densely packed aggregates and large void volumes between aggregates. Individual spheroids that can be resolved in the clusters appear to have a uniform size distribution.

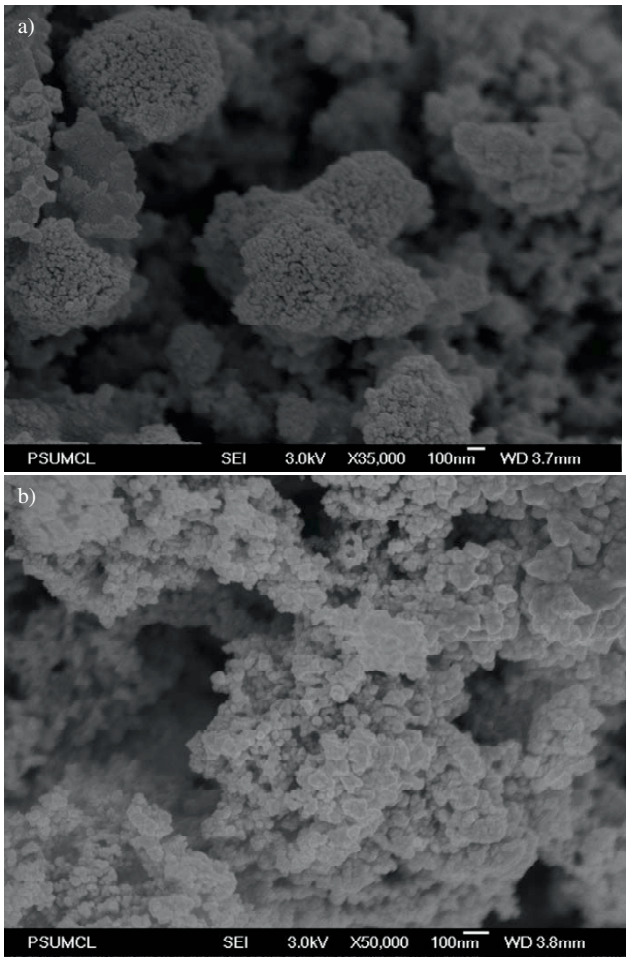

Figure 3
FESEM images of deposits formed at the tip of HP-fuel injector nozzles at varying magnifications.

Polished sections of the deposits examined with a polarized-light microscope also show aggregates of densely packed spherical particles (Figure 4). Different colors observed on the polarized-light micrographs in Figure 4 result from differences in reflectance of polarized-light depending on the porosity (or bulk density) of the aggregates. All aggregates examined under the polarized-light exhibited an isotropic texture, as was observed in the deposits from jet fuel thermal oxidative degradation [3]. The flat edges in the particles seen in Figure 4c and 4d show that they were in contact with a substrate- in this case, the fuel injector tip. The spherical morphology of the deposits suggests that they were formed in the liquid phase, deposited on the tip and aggregated into dense clusters. The presence of significant porosity between clusters (or absence of massive solid structures on the substrate) also support the inference that the particles nucleated and grew in the fluid phase and deposited onto the substrates to form the aggregates.

TEM of the HPDI deposits (Figure 5) also confirm that they consist of aggregated particles that form condensed structures. Figures 6a and 6b show the HRTEM images of a single particle at different magnifications. Unlike the jet fuel deposits, the individual particles of HPDI deposits show no regions of layer plane alignment in their internal structures. This suggests that the fraction of

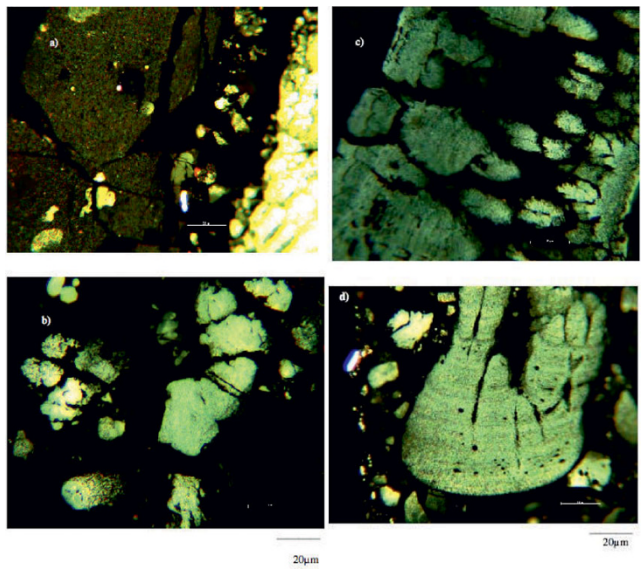

Figure 4
Polarized-light microscopy images of HPDI deposits.

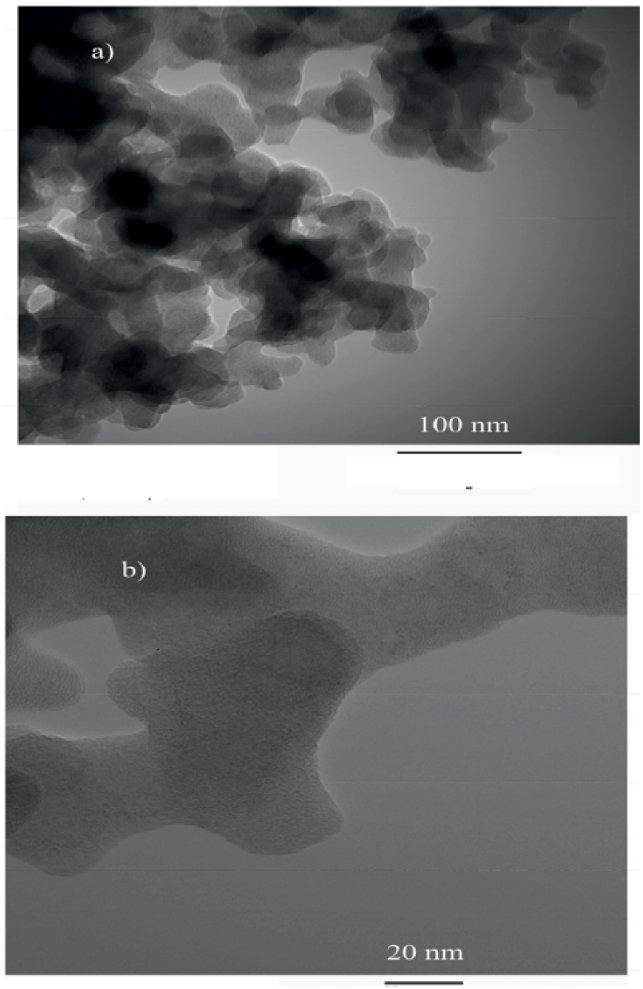

Figure 5
TEM image of deposits from HPDI at varying magnification.

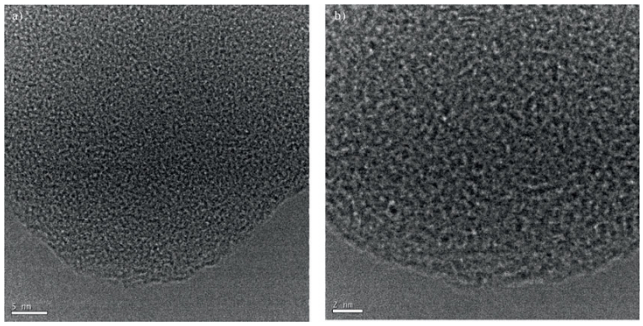

Figure 6
(a) HRTEM images of deposits obtained from HPDI at a magnification of 1 × 10^6×. (b) HRTEM image of deposits obtained from HPDI at a magnification of 500, 000×.

disordered structures in these deposits may be much higher than in those formed from jet fuel degradation.

Spectroscopic analysis of deposits

DRIFTS

The spectrum in Figure 7 shows the chemical groups present in the commercial HPDI deposits. The bands at 1600 cm^{-1} and 1735 cm^{-1} are assigned to the aromatic carbon-carbon stretch and C = O groups, respectively. The peak ~1200 cm^{-1} corresponds to C-O groups. The presence of C = O and C-O linkages indicate the presence of carboxylic acid, lactone or carboxylic anhydride groups in the deposits. Sauer et. al. [7] in their study of sediment formation from the degradation of heating oils, suggested the presence of oxygen functional groups in the form of ester type linkages in the deposits.

The peaks between 700 and 900 cm^{-1} (out of plane bending of aromatic H) indicate the substitution of aromatic-H by other functional groups. The peaks at 893 cm^{-1}, 838 cm^{-1} and 760 cm^{-1} are assigned to isolated aromatic H, two adjacent aromatic H, and 4 adjacent aromatic H respectively [8]. Low intensity of these peaks indicates these deposits are comprised of condensed polyaromatic hydrocarbons. The broad band between 2900 and 3600 cm^{-1} corresponds to -OH stretch [9, 10]. This is a combination of the -OH groups in phenolic compounds as well as water adsorbed on the KBr powder.

The bands at 3050 cm^{-1}, 2970 cm^{-1} and 2850 cm^{-1}which correspond to the aromatic C-H stretch, $-CH_3$ asymmetric stretch and $-CH_2$ stretch, respectively, are weak. The low intensity of the aromatic C-H peak at 3050 cm^{-1} is attributed to a relatively high oxygen concentration in the deposits [11]. The weak $-CH_2$, $-CH_3$ bands suggest that the aliphatic groups associated with the deposits are

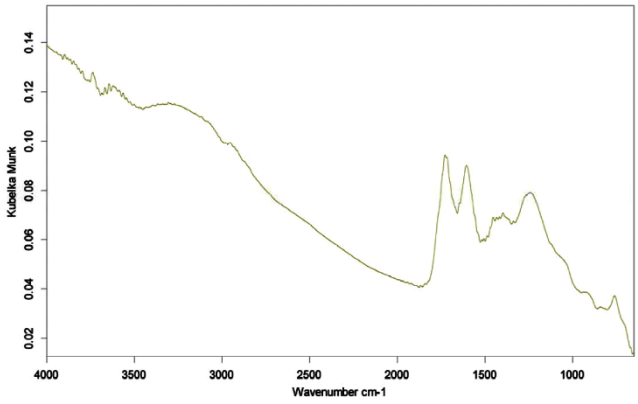

Figure 7
DRIFTS spectrum of HPDI deposits.

negligible. Comparison of the IR spectrum of diesel injector deposits to the IR spectra of the deposits from Jet A thermal oxidative degradation suggests they have a similar chemical composition – condensed polyaromatic structures with single and double bonded oxygen moieties.

X-ray photoelectron spectroscopy

The XPS spectrum of the injector deposits is shown in Figure 8a. The binding energy (BE) values of all the peaks in the spectrum were corrected by a charge correction factor corresponding to C 1s peak at 284.7 eV. The XPS spectrum showed only the presence of C and O on the surface of the deposits. The O/C ratio in the deposits was determined to be ~0.2. This is in the same range as the O/C ratio seen in the deposits formed from jet fuel thermal oxidative degradation. The high resolution C 1s spectrum obtained from these deposits is shown in Figure 8b. This showed three distinguishable components with peaks at 284.7 eV, 286.5 eV and 288.8 eV, respectively. The peak at 284.7 eV corresponds to Ar(C) [12]. This complements the results from DRIFTS analysis of the deposits indicating polyaromatic hydrocarbons.

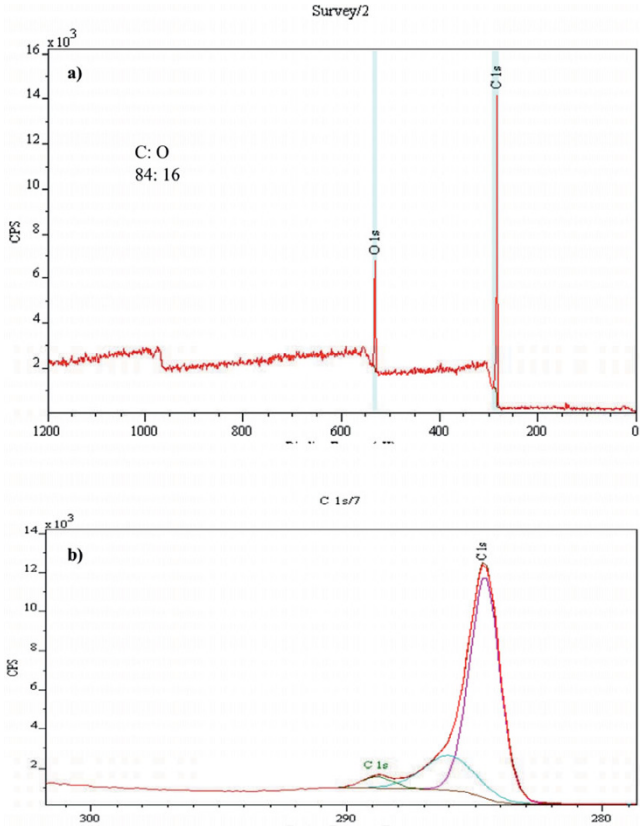

Figure 8
(a) XPS spectrum of HPDI deposits. b) High Resolution C 1s spectrum of the same.

The peak at 286.5 eV is assigned to C-O. C-O groups indicate the presence of phenolic, furan, alcohol or ether groups. The peak at 288.8 eV is assigned to a $\begin{matrix} C{=}O \\ | \\ O \end{matrix}$. This peak supports the results obtained from the DRIFTS analysis of the deposits indicating the presence of oxygenated groups such as carboxylic acids, anhydrides or lactones on the deposits [13-15]. The TPO and TGA-MS analysis of the deposits, discussed in section 5.4.4 gave information on their chemical reactivity and hydrogen content.

Temperature Programmed Oxidation (TPO) analysis

We see from the TPO profile in Figure 9a that the CO_2 evolution from the HPDI deposits occurred over a wide temperature range (150–750°C). The CO_2 evolved between 150–200°C is due to the oxidation of lighter hydrocarbons physisorbed on the deposits. The CO_2 peak at 580°C is attributed to the oxidation of polyaromatic hydrocarbons. The temperature of CO_2 evolution from this component of the HPDI deposits is similar to that of the less ordered polyaromatic components of the jet fuel deposits. This suggests that

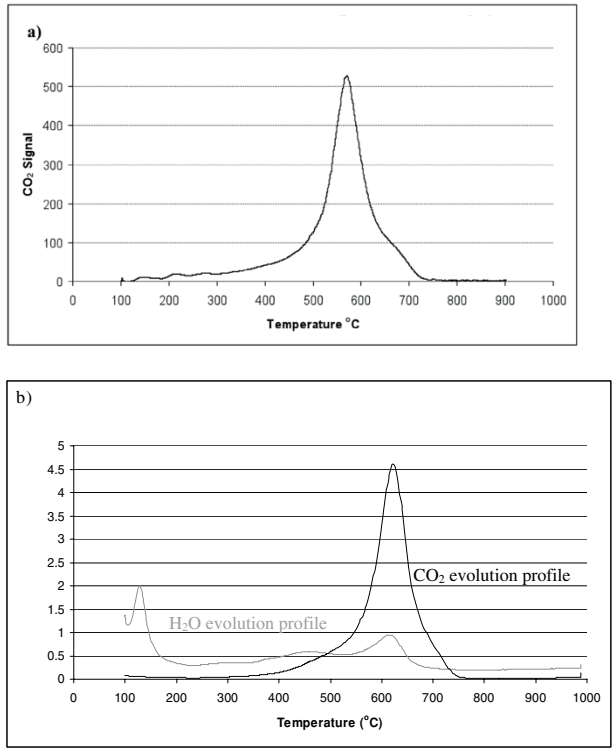

Figure 9
(a) TPO profile of HPDI deposits. (b) TGA-MS profile of CO_2 and H_2O evolved from the oxidation of carbon and hydrogen species in HPDI deposits from 100–1000°C.

the structural order and corresponding oxidation reactivity of this component of the deposits from the two fuels is similar. Further evidence in this regard is obtained from the H_2O evolved from the HPDI deposits, as discussed in the next section. This also suggests that the shoulder near 680°C may be from the oxidation of more ordered polyaromatic components of the deposits.

TGA-MS analysis

The CO_2 evolution profile (Figure 9b) from the TGA-MS analysis of the HPDI deposits was similar to their TPO profile. Oxidation began around 350°C and was completed by 750°C. The carbon species bonded to the oxygen moieties are expected to be the most reactive components of the deposits, thus being the earliest to oxidize. The CO_2 evolution from disordered and relatively ordered polyaromatic structures occurred around 610°C and 720°C respectively. The shift in the CO_2 evolution peaks to lower temperatures in the TPO as compared to the TGA-MS can be attributed to the differences in heating rate and oxidant flow rate in the two techniques [16].

The H_2O evolution profile in Figure 9b shows three peaks, the first one < 200°C, the second at 450°C and the third at 600°C. The peaks at 120°C can be attributed mostly to the removal of physisorbed water from the deposits and to a small extent to the oxidation of physisorbed hydrocarbons on the deposits. The peaks at 450°C and 610°C indicate hydrogen released from the decomposition of hydroxyl groups and the hydrogen associated with the polyaromatic hydrocarbons respectively [17]. An H/C ratio of ~0.4 was obtained from the TGA-MS analysis of these deposits also indicating condensed polyaromatic rings. The high temperature shoulder at 720°C does not have a corresponding H_2O peak. This indicates that this component of the deposits do not have a significant amount of hydrogen associated with them. This corroborates with the well-known fact that structurally ordered solids have very little hydrogen associated with them. A similar trend was observed with the jet fuel thermal oxidative deposits as well [3].

Results from the thermal oxidative stressing of the diesel range model compound n-hexadecane are discussed in following section.

Characterization of deposits from the thermal oxidative degradation of n-hexadecane

Thermal stressing of n-hexadecane at 160°C and 450 psi in a flow reactor produced a relatively small amount of deposits (0.003 wt% of fuel mass flowed through the reactor in 2.5 h.) of thermal stressing. Figure 10 shows the TEM images of deposits formed from the thermal oxidative degradation of n-hexadecane at varying magnifications. The observed spherical morphology once again (Figure 10a), shows deposit nucleation and growth in the fluid phase. The internal structure of the individual spheres was revealed at higher magnifications (Figures 10b and 10c). While the interior of the deposits seemed to contain amorphous carbonaceous material, parallel lattice fringes were observed towards the outer

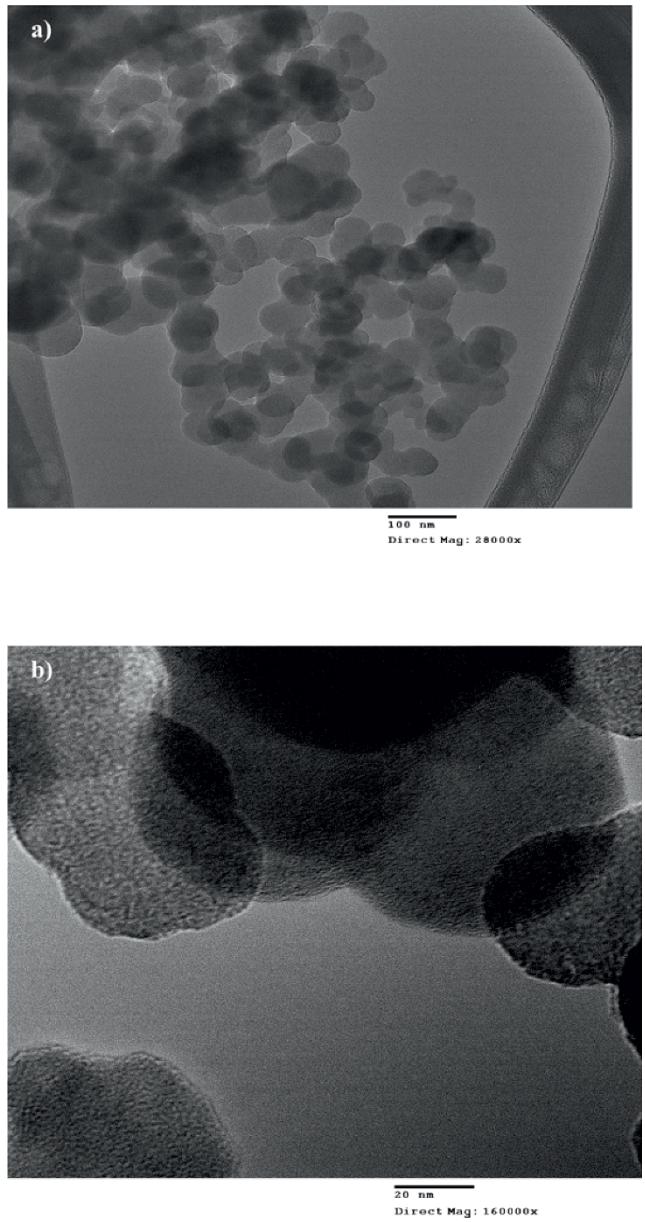

Figure 10
TEM images of deposits formed from the thermal oxidative degradation of n-Hexadecane at 160°C and 450 psi for 2.5 h at magnifications of (a) 24,000× (b) 160,000 × and (c) 350,000×.

portions. These fringes show layers of planar polyaromatic structures. Comparing Figures 10 and 6 one can say that, the structure of the deposits formed from n-hexadecane was similar to those formed from the HPDI with the main difference being a higher fraction of ordered carbonaceous material in the deposits formed from n-hexadecane. The reason for this observation is explained below. This suggests that the HPDI deposits will show a higher oxidation reactivity compared to the n-hexadecane deposits.

The DRIFTS spectrum of the n-hexadecane deposits diluted with KBr is shown in Figure 11. The weak DRIFTS signal is indicative of the high carbon content in the deposits due to which most of the incident IR is absorbed. The most prominent peak seen is the aromatic (C = C) stretching band at 1600 cm^{-1}. Weak bands compared to those seen in the DRIFTS spectrum of HPDI deposits were observed near 1735 cm^{-1} and 1200 cm^{-1} corresponding to C = O and C-O groups respectively. This shows that although the deposits contain some oxygen species, their concentration is relatively low.

During TGA-MS analysis, the peak CO_2 evolution from the hexadecane deposits occurred around 740°C (Figure 12). This is 20°C higher than the temperature of CO_2 evolution from the ordered structures in the HPDI deposits. This result agrees with the observation in the TEM images of the two deposits where a higher degree of structural order was seen in the n-hexadecane deposits compared to the deposits formed from the thermal oxidative degradation of diesel. The higher structural order in the deposits formed from n-hexadecane compared to those from diesel can be attributed to differences in hydrocarbon composition. Past studies

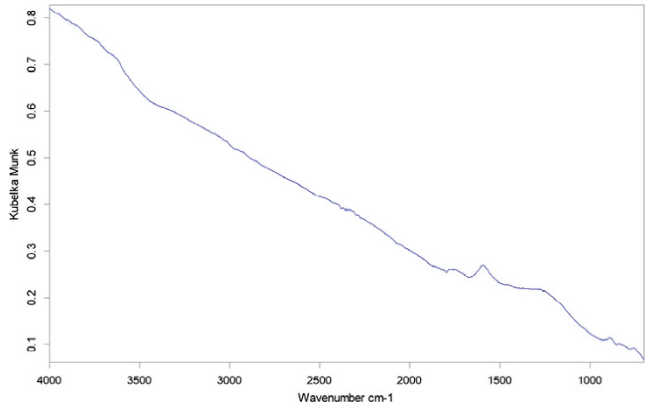

Figure 11
DRIFTS spectrum of deposits formed from the thermal oxidative degradation of n-Hexadecane at 160°C and 450 psi for 2.5 h.

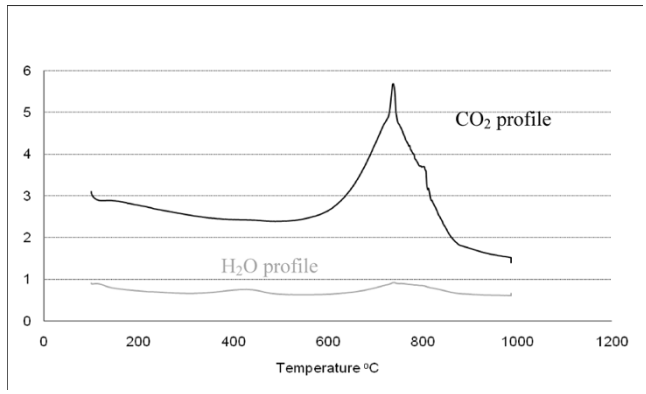

Figure 12
TGA-MS profile of CO_2 and H_2O evolved from the oxidation of solid deposits formed from n-Hexadecane degradation from 100 – 1000°C in the oxidant stream.

have shown that carbonaceous solids formed from relatively large aromatic species have an amorphous structure due to growth by the coalescence mechanism [18] while the solids formed from smaller hydrocarbons (such as soot formed from acetylene) are comprised of more ordered graphitic structures due to controlled hydrogen abstraction-carbon addition (HACA) reactions [19]. Diesel being a complex blend of aliphatic, cycloalkane and aromatic compounds would tend to form more amorphous structures upon degradation compared to the solid products formed from relatively simple radicals originating from n-hexadecane.

The temperature range for CO_2 evolution from the n-hexadecane deposits was 540°C to 900°C. The CO_2 contribution from the most reactive component of the deposits, oxidizing around 450°C in the n-hexadecane deposits is not apparent (Figure 12) in its mass spectrometer profile. This was clearer in the TGA-MS profile of the HPDI deposits. In both cases however, the corresponding H_2O peak evolving around the same temperature can be observed. This suggests that the CO_2 peak evolving from the n-hexadecane deposits between 400 and 500°C may be hidden by the offset in the baseline of the CO_2 evolution profile. This is due an instrumental effect and is explained in more detail in the study of the jet fuel degradation deposits [3].

The second H_2O peak evolving at 750°C can be attributed to the hydrogen species associated the polyaromatic hydrocarbons. The spikes in the CO_2 evolution profile at 750°C and 800°C can be attributed to the oxidation of capsules of volatiles (comparable to volatiles present during micropore development in char) trapped within the layers of ordered polyaromatic hydrocarbons [20]. We see from Figure 12 that the

intensity of the H_2O evolution peak from these volatiles, although visible is significantly low. Such capsules were also observed in the TPO profiles of deposits formed from jet fuel degradation. The relatively low oxidation reactivity indicated by TGA-MS analysis of the n-hexadecane deposits corresponds to the low signal obtained from carbon rich deposits during DRIFTS analysis.

The formation of carbon rich deposits containing ordered polyaromatic structures from the thermal oxidative degradation of n-hexadecane shows clearly that large polycondensed aromatic hydrocabons can be formed from paraffins at temperatures as low as 160°C in presence of oxygen.

GC/MS analysis of the liquid degradation products (discussed below) provides further evidence in this regard. Jensen and co-workers [21, 22] in their study of the liquid-phase oxidation of n-hexadecane proposed that the intermediate hydroxyl and alkylperoxy radicals formed during degradation aid in hydrogen abstraction from the alkane chains. The role of oxygen can thus be compared to that of a catalyst in facilitating low temperature aromatization of aliphatic hydrocarbons.

The products of n-hexadecane thermal oxidative degradation were diluted in a 50% pentane – 50% methanol mix. Their GC/MS spectrum is shown in Figure 13. The most likely assignments based on the fragmentation pattern of individual peaks obtained from mass spectrometry are listed in Additional file 2. Products such as toluene are direct evidence of chain breaking and aromatization reactions in presence of oxygen. GC/MS analysis of the neat hexadecane before thermal oxidative stressing was done to ensure that there were no lighter hydrocarbon contaminants. In this experiment as with earlier ones on the liquid phase product distribution from jet fuel, oxygenated compounds such as alcohols, ketones, aldehydes and carboxylic acids of varying alkyl chain lengths were obtained. The thermal oxidative degradation of C_{16} alkanes yielded products with carbon numbers both smaller (C_4 – C_{15}) and larger (C_{17}+) than the parent molecule. The products such as alcohols, carbonyls and carboxylic acids are believed to be secondary products obtained from the rapid conversion of alkyl hydroperoxides [21]. Jensen and co-workers also proposed a scheme for the cyclization of oxygenated straight chain intermediates during oxidative degradation of n-hexadecane between 120 and 180°C. However, the cyclic compounds thus formed have oxygen atoms incorporated in the rings. The mechanism of formation of cycloalkanes from oxygen containing cyclic compounds at these low temperatures is not clear.

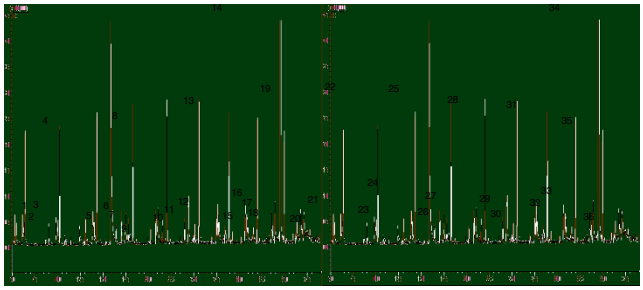

Figure 13
GC/MS chromatogram of 50% pentane – 50% methanol solubles from n-Hexadecane oxidative degradation at 160°C and 450 psi for 2.5 h.

The literature so far accounts for the presence of cycloalkanes, furans and their derivatives in the degradation products. However, the results presented here show that the solid deposits are primarily aromatic. A mechanism for oxygen assisted aromatization of the cycloalkanes has been proposed. The mechanism of formation of the alkylperoxy and alkoxy radicals which are the proposed hydrogen scavengers has already been described by Jensen and co-workers [23]

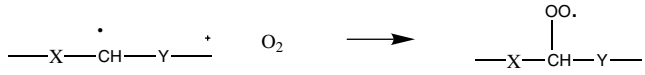

Hydrogen abstraction from cylcolkanes is a well known phenomenon [24]. The mechanism for hydrogen abstraction from cycloalkanes by alkylperoxy and alkoxy radicals has been proposed based on the above two steps.

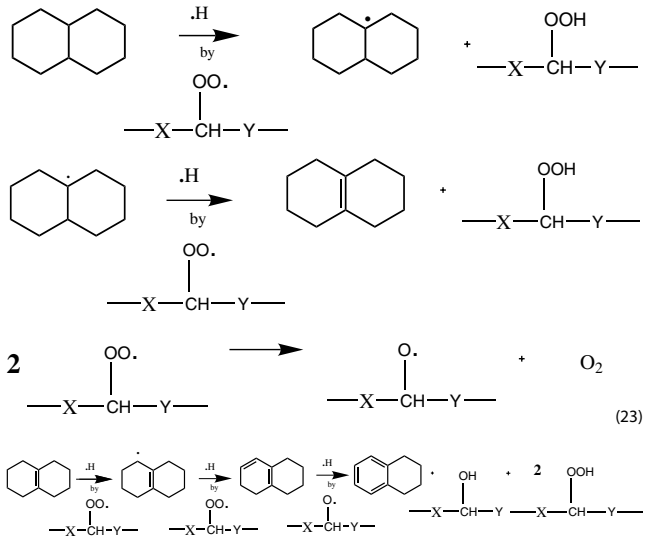

The mechanism proposed above shows the conversion of a cylcoalkane to a hydroaromatic compound. This can be considered the initial step in the aromatization of

cycloalkanes. As the hydrogen abstraction by alkylperoxy and alkoxy radicals proceeds, the aromatic compounds progressively undergo condensation and polymerization to form large PAHs. The amount of oxygen supplied in these experiments was calculated to be in excess of the amount required to form solids at the reported conversion ratio according to this mechanism. How the cyclic oxygenated intermediates participate in the conversion of paraffins to cycloalkanes during the thermal oxidative degradation of the fuel is not clear. Once the cycloalkanes are formed however, PAH formation can increase rapidly due to dehydrogenation by the highly reactive oxygenated intermediates. Dehydrogenation reactions leading to the formation of aromatics from paraffinic compounds so far have been known to occur only at relatively high temperatures (> 400°C) in the absence of dehydrogenation catalysts [25]. The presence of aromatic solids at temperatures as low as 160°C suggest that the oxygenated intermediates are responsible for this phenomenon.

Conclusion

The chemical and morphological properties of HPDI deposits showed similarities in structure properties of those formed from the thermal oxidative degradation of a model compound, n-hexadecane in short duration experiments. These results suggest that the deposits formed at the tip of the diesel injector were also formed by oxidative degradation of diesel fuel under similar temperature-pressure conditions. Both kinds of deposits consist of polycondensed aromatic hydrocarbons arranged with varying degrees of structural order in the solid carbons. Both deposits also contained oxygenated functional groups.

Thermal oxidative stressing of n-hexadecane showed that aromatic solids can be produced from n-paraffins at temperatures as low as 160°C in presence of oxygen. Alkoxy and alkylperoxy intermediates, once formed during the thermal oxidative degradation of hydrocarbons may lead to the formation and aromatization of cycloalkanes by hydrogen abstraction at relatively low temperatures.

Experimental

Deposits formed at the tip of commercial high-pressure diesel injectors after at least hundreds of hours of operation were collected and characterized.

The surface morphology of the deposits was determined using Field Emission Scanning Electron Microscopy (FESEM). The morphology of the deposits was observed under very high magnifications (~100,000×). The FESEM used in this study was a JEOL 6700F located at the Materials Research Institute at Penn State.

The internal structure of the deposits was determined by polarized-light Microscopy (PLM), Transmission Electron Microscopy (TEM) and High Resolution Transmission Electron Microscopy (HRTEM).

Polished epoxy pellets were made up with the solid samples to examine their optical texture. A Nikon Microphot FXA-II polarized-light microscope was used for this purpose. A Philips TEM – 420ST Transmission Electron Microscopy (TEM) was used to study the nanostructure of the solid deposits. This was operated at 120 kV. The solid deposits were either scraped off the coupons or dispersed in alcohol and deposited onto a 200 mesh copper grid with a lacey carbon film.

Chemical characterization of the deposits was done using Diffuse Reflectance Infrared Fourier Transform Spectroscopy (DRIFTS), X-ray Photoelectron Spectroscopy (XPS) and Temperature Programmed Oxidation (TPO) and Thermo-Gravimetric Analyzer-Mass Spectrometer (TGA-MS).

DRIFTS provides information on the nature of hydrocarbon and heteroatom bonds in the deposits. The infrared spectrometer was used in the diffuse reflectance mode. An IFS 66/S high performance research grade FT-IR spectrometer equipped with the use of interchangeable optical components and an MCT detector located at the Materials Research Institute in Penn State was used. A Spectra-Tech Collector II DRIFTS accessory was used. 10 mg of deposits collected from the flow reactor were ground and mixed with 300 mg of ground KBr powder (placed in an oven at 100°C for at least 24 h). A minimum of 400 scans were made per sample.

XPS was used to obtain the chemical composition on the surface of the deposited substrates upto a depth of ~100 Å. The samples were analyzed in a Kratos Analytical Ultra 15 m spatial resolution monochomatic Al k x-ray source auto stage, autovalving sample rotation stage, UHV in situ sample preparation chamber XPS at the Materials Research Institute in Penn State. The analyses covered an area of 750 μm × 350 μm on the sample.

Temperature-Programmed Oxidation was done on the metal substrates after thermal stressing in a LECO RC-412 multiphase carbon analyzer. This technique involves exposing the sample containing carbonaceous material to a flowing O_2 gas/O_2-inert gas mixture stream in a furnace while increasing the temperature of the furnace from 100 to 900°C at constant heating rate of 30°C/min and holding it at 900°C for 300 s. A constant O_2 flow rate of 750 cc/min was used in all the analyses.

A TGA 2050 was used to determine the thermal weight loss curves of the solid deposits on the metal substrates. The gasification reactions were carried out in a 50% O_2/Ar mixture gas stream at a flow rate of 130 cc/min. The sample containing deposits was cut up into chips and placed in a porcelain refractory pan. The pan was then heated in a furnace from room temperature to 1000°C at a constant heating rate of 10°C/min. The weight change of the sample was recorded continuously during the analyses. The gaseous products from the gasification of the samples in the TGA were quantitatively analyzed using a mass-spectrometer.

The liquid soluble components extracted from the deposits after washing with pentane, toluene and methanol were analyzed by Gas Chromatography/Mass Spectrometry (GC/MS). A Shimadzu GC/MS was used. The samples were collected in 2 ml GC vials. A 1 μL injection volume was used. The following temperature-pressure profiles were used to generate tables in Additional files 1 and 2 respectively during the GC analyses of the samples: Additional file 1. Temperature profile: Initial temperature 40°C; Hold time – 4 min; Ramp – 15°C/min; Final temperature – 340°C/min; Final hold time – 15 min. Pressure profile: Initial pressure – 48.9 kPa; Hold time – 4 min; Ramp – 5.7 kPa/min; Final pressure – 162.4 kPa; Final hold time – 15 min. Solvent cut time – 2.4 min.

Additional file 2. Temperature profile: Initial temperature 40°C; Hold time – 4 min; Ramp – 4°C/min; Final temperature – 340°C/min; Final hold time – 5 min. Pressure profile: Initial pressure – 48.9 kPa; Hold time – 4 min; Ramp – 1.5 kPa/min; Final pressure – 162.4 kPa; Final hold time – 5 min. Solvent cut time – 5 min.

A Hewlett Packard Series II gas chromatograph 5890 pyrolysis GC/MS was used to analyze the solid components in the deposits.

A Waters Micromass Matrix Assisted Laser Desorption Ionization Time of Flight (MALDI-TOF) mass spectrometer was used to determine the molecular weight distribution of the HPDI deposits. MALDI experiments are carried out by pulsing a Nitrogen UV laser (337 nm wavelength) onto the sample. The UV laser light is absorbed and vaporizes small amounts of protonated, non fragmented ions, which are carried then into the gas phase. The MALDI-LR was operated in a positive reflectron mode in a mass range of 10 m/z to 3,000 m/z. 1.0 μL of each sample was spotted in a separate well on a 96 stainless steel well plate and air-dried. No matrix was used in the experiments.

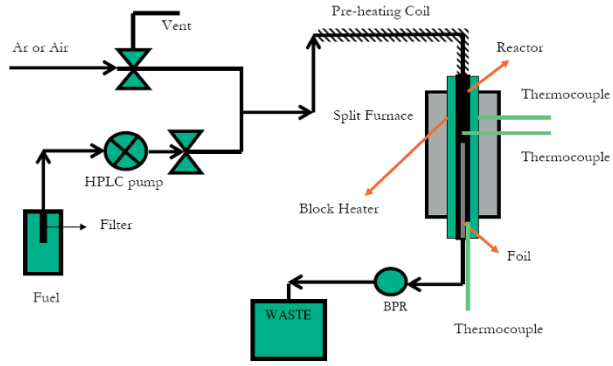

Figure 14
Schematic representation of the flow reactor set-up used to stress n-hexadecane.

A model compound, n-hexadecane was stressed in a flow reactor under thermal oxidative conditions. The reactor used was a 1/4 in (OD), 20-cm long, glass-lined, stainless steel tube reactor inserted in a vertical block heater. The temperature and pressure during thermal stressing were set at 160°C and 450 psi respectively. The start time for the experiment was noted after the bulk fuel temperature reached the wall temperature of 160°C. The fuel temperature and pressure were kept constant for the duration of the experiment. The thermal stressing was carried out for a period of 2.5 hr in the presence flowing air. The fuel flow rate into the reactor for the thermal stressing experiments was 1.2 mL/min and air flow was 50 mL/min. Both reactants followed a single-pass route. Based on the fuel flow rate and the reactor dimensions, the total residence time of the fuel in the reactor was calculated to be 77 s. Figure 14 is a schematic representation of the flow reactor set up used for the thermal oxidative stressing of n-hexadecane.

The liquid products obtained from the thermal oxidative degradation of n-hexadecane were analyzed in the Shimadzu GC/MS QP 5000. The solid deposits formed from the model compound were analyzed by TEM to determine their internal structure. DRIFTS, XPS, and TGA-MS were used to obtain information on the chemical composition and reactivity of the deposits.

Competing interests

The authors declare that they have no competing interests.

Authors' contributions

RV performed all the experiments, carried out the characterization of all the samples except the HRTEM and prepared the original draft of the manuscript.

SE supplied the coked injectors, initiated the work plan, provided feedback on the results and discussions and critically revised the manuscript for intellectual and written content.

Additional material

Additional file 1

Table 1. List of compounds seen in the GC/MS spectrum of methanol-pentane soluble fractions from diesel deposits.
Click here for file
[http://www.biomedcentral.com/content/supplementary/1752-153X-2-25-S1.doc]

Additional file 2

Table 2. List of compounds seen in the GC/MS spectrum of liquids obtained during the thermal oxidative degradation of n-hexadecane at 160°C for 2 h at a flow rate of 1.2 ml/min.
Click here for file
[http://www.biomedcentral.com/content/supplementary/1752-153X-2-25-S2.doc]

Acknowledgements

This work was part of the study on the 'Characterization of Deposits formed from the Pyrolytic and Oxidative Degradation of Jet Fuel and Diesel'. The authors are grateful to the contributions of the following people: Prof. L. Radovic, Dr. S. Pisupati and Prof. B. Santoro for their feedback and comments on the study; Josh Maeir and Dr. T. Clark at the Materials Research Institute at Penn State University for carrying out the HRTEM analysis of the samples; Arun Ram Mohan at The Energy Institute at Penn State University for providing MOCVD coated specimens for the study on jet fuel; Nicole Wonderling at the Materials Research Institute at Penn State for carrying out XRD analysis of samples from jet fuel; Rolls-Royce Corp. Indianapolis for funding Ramya Venkataraman's Ph. D. study.

References

1. Batts BD and Fathoni AZ: **A Literature-Review on Fuel Stability Studies with Particular Emphasis on Diesel Oil.** *Energy & Fuels* 1991, **5(1):**2–21.
2. Beaver B, Gao L, Burgess-Clifford C and Sobkowiak M: **On the mechanisms of formation of thermal oxidative deposits in jet fuels. Are unified mechanisms possible for both storage and thermal oxidative deposit formation for middle distillate fuels?.** *Energy & Fuels* 2005, **19(4):**1574–1579.
3. Venkataraman R and Eser S: **Characterisation of solid deposits from the thermal-oxidative degradation of jet fuel.** *International Journal of Oil, Gas and Coal Technology* 2007, **1(1/2):**126–137.
4. Watkinson AP and Wilson DI: **Chemical reaction fouling: A review.** *Experimental Thermal and Fluid Science* 1997, **14(4):**361–374.
5. National Institute of Standards and Technology (NIST) compounds database..
6. Personal communication – Dr. Robert Minard, Prof. Emiretus, Department of Chemistry, Penn State University, UP 16802..
7. Sauer RW, Weed AF and Headington CE: *Proceedings of the American Chemical Society, Div. of Petroleum Chemistry symposia* 1958, **3(3):**95–113.
8. Eser S: **Mesophase and pyrolytic carbon formation in aircraft fuel lines.** *Carbon* 1996, **34(4):**539–547.
9. Sobkowiak M and Painter P: **Determination of the aliphatic and aromatic CH contents of coals by Ft-Ir – studies of coal extracts.** *Fuel* 1992, **71(10):**1105–1125.
10. Sobkowiak M and Painter P: **A comparison of drift and Kbr pellet methodologies for the quantitative-analysis of functional-groups in coal by infrared-spectroscopy.** *Energy & Fuels* 1995, **9(2):**359–363.
11. Solomon PR and Carangelo RM: **FT-IR analysis of coal 2. Aliphatic and aromatic hydrogen concentration.** *Fuel* 1988, **67:**.
12. XPS handbook Moulder JF, Stickle WF, Sobol PE and Bomben KD: **Handbook of X-ray Photoelectron Spectroscopy.** *Perkin Elmer Corp* Jill Chastain 1992.
13. Figueiredo JL and Trimm DL: **Carbon Formation on Unsupported and Supported Nickel Catalysts.** *Journal of Applied Chemistry and Biotechnology* 1978, **28(9):**611–616.
14. Rodriguez-Reinoso F and Molina-Sabio M: **Textural and chemical characterization of microporous carbons.** *Advances in Colloid and Interface Science* 1998, **77:**271–294.
15. Bleda-Martinez MJ, Lozano-Castello D, Moarallon E and Cazorla-Amoros D: **Chemical and electrochemical characterization of porous carbon materials.** *Carbon* 2006, **44(13):**2642–2651.
16. Eser S, Venkataraman R and Altin O: **Utility of Temperature Programmed Oxidation for Characterization of Carbonaceous Solids from Heated Jet fuel.** *Industrial and Engineering Chemistry Research* 2006, **45(26):**8956–8962.
17. Aso H, Matsuoka K and Tomita A: **Quantitative analysis of hydrogen in carbonaceous materials: Hydrogen in anthracite.** *Energy & Fuels* 2003, **17(5):**1244–1250.
18. Lewis IC: **Chemistry of Carbonization.".** *Carbon* 1982, **20 (6):**519–529.
19. Frenklach M and Wang H: **Aromatics Growth Beyond the 1st Ring and the Nucleation of Soot Particles.** *Proceedings of the Combustion Institute* 1991, **23:**1559.
20. Boehman AL, Song J and Alam M: **Impact of biodiesel blending on diesel soot and regeneration of particulate filters.** *Energy and Fuels* 2005, **19(5):**1857–1864.
21. Jensen RK, Korcek S, Mahony LR and Zinbo M: **Liquid-Phase Autoxidation of Organic-Compounds at Elevated-Temperatures. 1. Stirred Flow Reactor Technique and Analysis of Primary Products from Normal-Hexadecane Autoxidation at 120-Degrees-C 180-Degrees-C.** *Journal of the American Chemical Society* 1979, **101(25):**7574–7584.
22. Jensen RK, Korcek S, Mahony LR and Zinbo M: **Formation, Isomerization, and Cyclization Reactions of Hydroperoxyalkyl Radicals in Hexadecane Autoxidation at 160–190-Degrees-C.** *Journal of the American Chemical Society* 1992, **114 (20):**7742–7748.
23. Jensen RK, Korcek S, Mahony LR and Zinbo M: **Liquid-Phase Autoxidation of Organic-Compounds at Elevated-Temperatures. 2. Kinetics and Mechanisms of the Formation of Cleavage Products in Normal-Hexadecane Autoxidation.** *Journal of the American Chemical Society* 1981, **103(7):**1742–1749.
24. Song CS, Eser S, Schobert HH and Hatcher PG: **Pyrolytic Degradation Studies of a Coal-Derived and a Petroleum-Derived Aviation Jet Fuel.** *Energy & Fuels* 1993, **7(2):**234–243.
25. Greensfelder BS, Voge HH and Good GM: **Catalytic and thermal cracking of pure hydrocarbons: Mechanisms of Reaction.** *Industrial and Engineering Chemistry Research* 1949, **41:**2573.